




Article

Potential Sites for Underground Energy and CO₂ Storage in Greece: A Geological and Petrological Approach

Apostolos Arvanitis ¹, Petros Koutsovitis ^{2,*}, Nikolaos Koukouzas ³, Pavlos Tyrologou ³,
Dimitris Karapanos ³, Christos Karkalis ^{3,4} and Panagiotis Pomonis ⁴

¹ Hellenic Survey of Geology and Mineral Exploration (HSGME), 13677 Attica, Greece; arvanitis@igme.gr

² Section of Earth Materials, Department of Geology, University of Patras, GR-265 00 Patras, Greece

³ Centre for Research and Technology, Hellas (CERTH), 15125 Marousi, Greece; koukouzas@certh.gr (N.K.); tyrologou@certh.gr (P.T.); karapanos@certh.gr (D.K.); karkalis@certh.gr or chriskark@geol.uoa.gr (C.K.)

⁴ Department of Mineralogy and Petrology, Faculty of Geology and Geoenvironment, National and Kapodistrian University of Athens, Zografou, P.C. 15784 Athens, Greece; ppomonis@geol.uoa.gr

* Correspondence: pkoutsovitis@upatras.gr; Tel.: +30-26-1099-7598

Received: 9 April 2020; Accepted: 25 May 2020; Published: 28 May 2020



Abstract: Underground geological energy and CO₂ storage contribute to mitigation of anthropogenic greenhouse-gas emissions and climate change effects. The present study aims to present specific underground energy and CO₂ storage sites in Greece. Thermal capacity calculations from twenty-two studied aquifers (4×10^{-4} – 25×10^{-3} MJ) indicate that those of Mesohellenic Trough (Northwest Greece), Western Thessaloniki basin and Botsara flysch (Northwestern Greece) exhibit the best performance. Heat capacity was investigated in fourteen aquifers (throughout North and South Greece) and three abandoned mines of Central Greece. Results indicate that aquifers present higher average total heat energy values (up to $\sim 6.05 \times 10^6$ MWh_(th)), whereas abandoned mines present significantly higher average area heat energy contents (up to $\sim 5.44 \times 10^6$ MWh_(th)). Estimations indicate that the Sappes, Serres and Komotini aquifers could cover the space heating energy consumption of East Macedonia-Thrace region. Underground gas storage was investigated in eight aquifers, four gas fields and three evaporite sites. Results indicate that Prinos and South Kavala gas fields (North Greece) could cover the electricity needs of households in East Macedonia and Thrace regions. Hydrogen storage capacity of Corfu and Kefalonia islands is 53,200 MWh_(e). These values could cover the electricity needs of 6770 households in the Ionian islands. Petrographical and mineralogical studies of sandstone samples from the Mesohellenic Trough and Volos basalts (Central Greece) indicate that they could serve as potential sites for CO₂ storage.

Keywords: underground; energy storage; natural gas; carbon storage; hydrogen; thermal energy; CO₂

1. Introduction

The use of fossil fuels as energy sources is one of the major contributors of anthropogenic greenhouse gas emissions that include CO₂ [1–3]. To mitigate the effects of global warming the implementation of CO₂ Capture and Storage (CCS) practices is considered as a state-of-the-art technology that aims to reduce emissions of CO₂ into our living atmosphere [4]. To achieve efficient and sustainable energy management it is important to promote practices that aim to reduce the carbon footprint through utilisation of renewable energy resources (wind, biomass, solar and geothermal energy) in Greece with integration of energy storage concepts [5]. This can be achieved with gradual transition to eco-friendly energy systems that promote energy production with the inclusion of Renewable Energy Sources utilisation. This energy transition presents significant and important

developments, such as the geothermal energy exploitation in Kenya [6]. However, their global contribution in total renewable energy production is small. This is attributed to the obvious difficulties that are linked with the supply of renewable sources. In the current stage, even more countries tend to adapt and promote the use and research on renewable energy sources [7].

More specifically, energy storage applications as a concept aim to provide technologies that convert energy into storable forms [8]. It also balances energy consumption with production by storing excess energy for long and/or short periods [9]. Despite the cover of energy demands (i.e., seasonal, daily), energy storage provides additional benefits such as: decrease of operational costs, integration of variable energy sources (such as wind, solar, natural gas and geothermal energy) and reduction of environmental effects (low carbon energy supply). Supplementary energy conversion processes are often required, depending on the source type and the implemented storage technology. Energy storage systems can be distinguished into mechanical, chemical, biological, magnetic, thermal and thermochemical types [10]. The choice of the appropriate storage technology depends on the storage purpose, the type of energy source the available storage capacity cost, lifetime and environmental impact [8]. Energy storage systems are distinguished into ground (ground-based ex-situ) and underground (geological in-situ) types. Underground energy storage requires suitable geological reservoirs such as: depleted hydrocarbon reservoirs, rock bodies with appropriate lithotypes (ultramafic rocks, basalts and sandstones), deep saline aquifers, salt caverns and abandoned mines.

Underground Thermal energy storage systems (UTES) provide the opportunity to store thermal energy, by utilising the heat capacity of underground soil and/or rock volumes [11]. To date, the best-established types of seasonal UTES systems [12,13] are aquifer storage (ATES), borehole storage (BTES), cavern storage (CTES), pit storage (PTES) and seasonal tank storage (TTES). There are many specific localities with potential for underground energy storage in Greece [14]. Aquifers for seasonal underground heat or natural gas storage are in sedimentary basins of the Greek mainland (such as Thessaloniki basin; North Greece), as well as in the Aegean islands (such as Evia, Lesbos, Chios and Rhodes). Natural gas can be sufficiently stored in depleted natural gas reservoirs that exist in Greece (Figure 1), which are selected on the basis of a sufficiently large volume of pore space, preferably high permeability of reservoir rocks and the absence of gas admixtures such as hydrogen sulphides. Hydrocarbon reservoirs that could serve as potential sites for underground gas storage include those of Epanomi (Thessaloniki, North Greece), Katakolo (South Greece) and Prinos (North Greece) [14].

Apart from the aforementioned, hydrogen is considered nowadays as an important key source for clean, secure and affordable energy, since it can improve efficiency of power systems and reduce environmental impact of power production [15]. Hydrogen can be stored into porous reservoir rocks such as depleted natural gas or petroleum deposits [16] and salt caverns [16,17]. In Greece, the most suitable formations for considering hydrogen storage (Figure 1) are the caverns in salt/evaporite formations due to the fact that they allow higher injection and withdrawal rates compared to other means of storage [18] thus resulting in high energy deliverability to the energy grid. Evaporite formations of Heraklion (Crete Island; South Aegean) are suitable for underground gas storage, whereas Corfu and Kefallonia Islands (Ionian Sea) could serve as sites for underground hydrogen storage. The abandoned mines of Mandra and Chaidari regions (Attica; Central Greece), as well as the Aliveri mine (Evia Island; Central Greece) could be exploited for underground heat storage purposes.

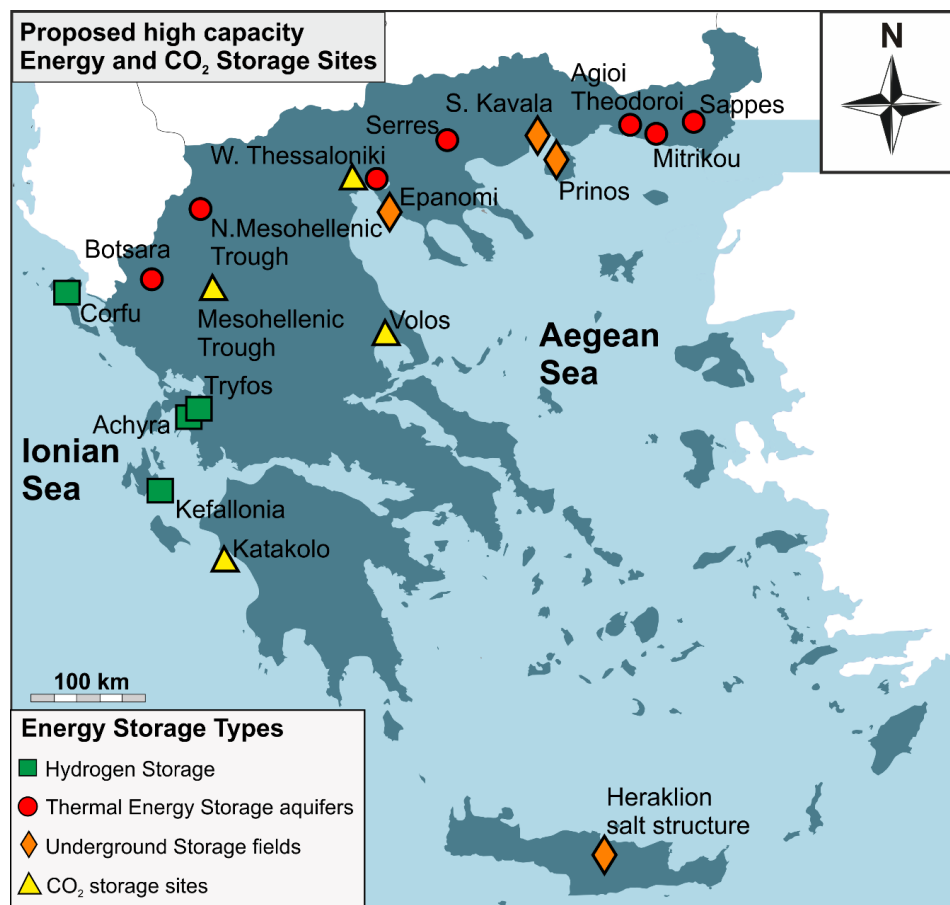


Figure 1. Main proposed high capacity energy and CO₂ storage sites (hydrogen storage: 26,600 MWh_{el}; Thermal Capacity: 2930–4651 MJ; Gas Storage Capacity: 928,097–4,826,105 MWh_{el}; CO₂ storage: 27,600 t [3] to 1350 Mt [19]).

Several research studies have developed effective methods for carbon capture, by utilising technologies such as membranes, adsorption-based separation of CO₂ [20]. There are many options for Geological CO₂ storage such as deep saline formations [21], abandoned coal mines [22], salt caverns [23], coal seams [24] and depleted hydrocarbon fields [25]. In many cases, CO₂ storage can be combined with extraction of crude oil (CO₂-Enhanced Oil Recovery [26]) or natural gas from hydrocarbon reservoirs (CO₂-Enhanced Gas Recovery). Mineralisation is an alternative option of CO₂ sequestration. Several rock types have been considered as potential underground reservoirs for mineral storage of carbon, or to withhold for a relatively short period of time specific amounts of CO₂. These include: (a) basalts with high porosity, silica undersaturated nature, abundance of plagioclase and feldspars and low alteration grade (recent age) [3,27,28], (b) sandstones [29,30] and (c) serpentinite bodies [31,32].

The most common parameters that must be considered prior to the implementation of CO₂ storage in the aforementioned formations include, the storage capacity, porosity and permeability of the reservoir rock. In addition, the possibility of CO₂ leakage or defects associated with cement degradation must be examined prior to CO₂ storage in cases of depleted hydrocarbon reservoirs [33]. The possibility of migration of the injected CO₂ and/or brine into the drinking water zones is a major concern that must be taken into account in the case of deep saline aquifers [21]. The absence of lateral communication with other mines and/or with the surface (to avoid gas leakage), as well as the minimum depth of the mine top are crucial parameters for CO₂ storage in abandoned coal mines [34]. Regarding the CO₂-mineralisation in rocks, the abundance of Ca–Fe–Mg bearing minerals significantly affects the amount of carbonate minerals produced during reaction of the rock with the injected CO₂ [3].

At the current stage Greece has not developed and adopt significant CO₂ storage sites and policies, while there are only few studies concerning the application of Carbon Capture and Storage (CCS) technologies in this region [35]. In Greece, the regions of Volos (Figure 1) [3], the Mesohellenic Trough [29], the Prinos oil and gas field (Kavala; North Greece) and also parts of Western Greece [36] encompass the appropriate rock types that could serve as potential sites for CO₂ storage. Preliminary estimations of CO₂ storage in Volos basalts indicate storage capacity of ~43,200 tons CO₂ at 300 m depth [3]. Calculations conducted by [37] present high storage capacity of CO₂ in the Pentalofos and Eptachori sedimentary formations of the Mesohellenic Trough at 2 and 3 km depths, respectively. Calculations of CO₂ storage at Klepa-Nafpaktia sandstones in Western Greece indicate storage capacity of 18×10^5 tons of CO₂ at 500 m depth [36]. Additional study indicates that ultramafic rocks from Vourinos ophiolite complex (Western Macedonia; North Greece) could be used for CO₂ sequestration purposes [38].

The present study aims to present, map and investigate specific underground energy storage sites that can be considered to potentially utilise Underground Thermal Energy Storage (UTES), Underground Gas Storage (UGS), Hydrogen and CO₂ underground storage practices in Greece. For this purpose, we considered data derived from petrological and geochemical assessments, field observations and referenced data from extensive literature review, but also through the application of energy storage calculations that take into consideration the physicochemical properties of the potential reservoirs. In this framework, we aim to revise and upgrade preliminary research results provided by [39].

2. Analytical Techniques

Preliminary results of the selective surface rock samples from several parts of the Mesohellenic Trough and the region of Volos have been examined regarding their petrographic properties. Four sandstone samples were collected from the regions between Deskati and Doxiana near Grevena and one sandstone sample was collected from the Lignite Center of Western Macedonia near Ptolemais. Three basaltic rock samples were examined from the regions of Microthives and Porphyrio near Volos. XRD analyses were conducted at CERTH's (Centre for Research and Technology, Hellas) Laboratories, using a Philips X'Pert Panalytical X-ray diffractometer (Malvern Panalytical, Malvern, UK) that operates with Cu radiation at 40 kV, 30 mA, 0.020 step size and 1.0 s step time. Interpretation of XRD results, was accomplished by deploying the DIFFRAC.EVA software v.11 (Bruker, MA, USA), which is based on the ICDD (International Center for Diffraction Data) Powder Diffraction File (2006). Sandstone and basaltic rock samples were examined through petrographic observations in polished thin sections using a Zeiss Axioskop-40 (Zeiss, Oberkochen, Germany), equipped with a Jenoptik ProgRes CF Scan microscope camera at the Laboratories of CERTH. The modal composition of pores was calculated based upon ~1000-point counts on each thin section. Quantification of modal composition was accomplished by using microphotography of SEM images at CERTH's Laboratories with a SEM-EDS (Scanning Electron Microscopy with Energy Dispersive Spectroscopy) JEOL JSM-5600 scanning electron microscope (Jeol, Tokyo, Japan), equipped with an automated energy dispersive analysis system Link Analytical L300 (Oxford Instruments, Abington, UK), with the following operating conditions: 20 kV accelerating voltage, 0.5 nA beam current, 20 s time of measurement, and 5 µm beam diameter. The petrographic description of the sandstone and basaltic rock samples coupled with data provided by extensive literature review are presented below.

3. Geological Background and Petrological Investigation of Rock Types Considered for Storage

3.1. Evaporite Formations

In the Ionian and Pre-Apulian geotectonic zones, evaporites exhibit Triassic and Triassic–Lower Jurassic ages, respectively. The thrust boundary between the Ionian and pre-Apulian zones is marked by intrusion of evaporite occurrences, mostly after the effects of diapirism [40,41]. In the regions of Epirus and Akarnania (Western Greece), Triassic evaporites occur in various localities and in the central part

of the Corfu Island [42]. These occurrences provide proof that in the External Hellenides the evaporites represent the lowest detachment level of individual overthrust sheets [43]. Their thickness varies but in most cases is about 2–3 km, although locally it can reach up to 4 km [44–46]. Diapiric forms are usually observed in local scale, resulting in the deformation of the adjacent sedimentary rocks including those of Zavrohon diapir, that has also been confirmed by drilling boreholes [44]. Evaporite formations from Agios Sostis and Laganas regions in Zakynthos island (Western Greece) are represented by the Messinian evaporite unit [47]. These formations consist of nodular and banded evaporate minerals often being in contact with turbidite successions, whereas their formation is associated with present-day active tectonics [44,47].

The principal evaporite mineral phases that have been identified in the Greek evaporite formations are gypsum, halite and anhydrite [40,48]. On their upper stratigraphic levels, dolomite occasionally participates in the form of breccias, which is mostly observed in the Triassic formations. Accessory mineral phases include bassanite and celestite that are not always present. In Northwestern Greece, the porosity of evaporitic formations ranges widely from relatively impermeable to very permeable attributed to local karstification processes [49].

Triassic evaporites from the regions of Anthoussa and Agios Ioannis (West Greece) [50] indicate that these can be distinguished into two main types (Type-23 and Type-24) of Standard Microfacies based on the Flugel classification [51]. Both types are rich in dolomite and solution collapse breccia, whereas calcite, gypsum and anhydrite appear in notable but lower amounts [50]. Type-23 evaporites are laminated by layers of gypsum, anhydrite and dolomite. Dolomite ranges between 40%–60%, evaporite crystals are often calcified and form lenses and rosettes within the mudstone groundmass, whereas relic sparite and evaporite minerals are also observed [50]. Their secondary porosity ranges between 20%–30%. Type-24 evaporites are classified as dolomites and dolomitic limestones. Their depositional texture corresponds to mudstone-grainstone types [50]. Micritic cement is highly but not totally dolomitised, whereas sparitic material usually occurs as cementitious material [50]. Dolomite is present in high amounts reaching 80% [50]. Evaporite minerals reach ~20% and usually form rosette and lenses within the groundmass [50]. Secondary porosity ranges between 15%–40% [50].

Evaporite samples studied from different drilling depths at the region of Kristallopigi (Igoumenitsa; Western Greece) [49] include claystones and siltstones in the upper parts and organic rich evaporites with claystone intercalations in the lower parts. Their mineralogical composition is distinguished into evaporitic and non-evaporitic, including the following assemblages gypsum–anhydrite–bassanite–celestite and quartz–feldspar–calcite–dolomite–magnesite clays, respectively [49]. Clay minerals are classified as kaolinite, illite, smectite and mixed phases [49]. Regarding the evaporitic minerals gypsum is stressed and deformed presenting topotactic relation with bassanite crystals [49]. Bassanite is isolated or forms aggregates, whereas celestite is sub-idiotropic to tabular or prismatic forming aggregates or isolated crystals [49]. Porosity measurements show high variation between 0.31%–52.98% for the studied samples [49].

3.2. Sedimentary Basins

The Eocene-Miocene Mesohellenic Trough is an elongated sedimentary basin of 200 km length and 30–40 km width, located in NW Greece [52,53] between the Apulian (non-metamorphic) and the Pelagonian (metamorphic) microcontinental plates [54]. It is a back-arc sedimentary basin evolved during the Upper Oligocene to Miocene period [52,55–57], being superimposed on the Olonos-Pindos external and Pelagonian internal geotectonic units. It is the largest and most important molassic basin formed during the last Alpine orogenic stage of the Hellenides, which occurred between the Mid-Upper Eocene and the Mid-Upper Miocene, extending from Albania in the Northern parts, towards the Thessaly region in Greece at the South. The Mesohellenic Trough comprises of the following four main formations from downwards to surface: Eptachorio, Pentalofo, Tsotillio and Burdigalian [58]. The base of the Eptachorio Formation consists of clastic Upper Eocene to Lower Oligocene sediments (conglomerates, sandstones), as well as base deposits. The upper part of Eptachorio Formation (Figure 2a,b) is located

in Taliaros Mountain (Grevena-Kastoria; West Macedonia) and appears in the form of local sedimentary phases comprising of sandstones, marls and limestones. The sequence presents thickness varying from 1000 to 1500 m. The Upper Oligocene to Lower Miocene Pentalofos Formation (Figure 2a,b) includes two types of clastic sedimentary rocks separated by marl–sandstone intercalations. Their thickness ranges from 2250 to 4000 m. The Tsotillio Formation (Lower to Middle Miocene) consists of marls accompanied by conglomerates, sandstones and limestones of variable thickness (200 to 1000 m). The Burdigalian Formation comprises of various phases of sediments such as sandy and silty marls, sand clays, sandstones, conglomerates and limestones [37,52,54]. These sediments are deposited in the form of sedimentary wedges. The aforementioned formations are covered from: (a) Upper Eocene to Middle Miocene alluvial, lacustrine and terrestrial sediments and (b) Pliocene to Lower Pleistocene, fluvial and lacustrine clays, sands and loose conglomerates hosting lignite horizons, which in cases were deposited locally in the Mesohellenic Trough.

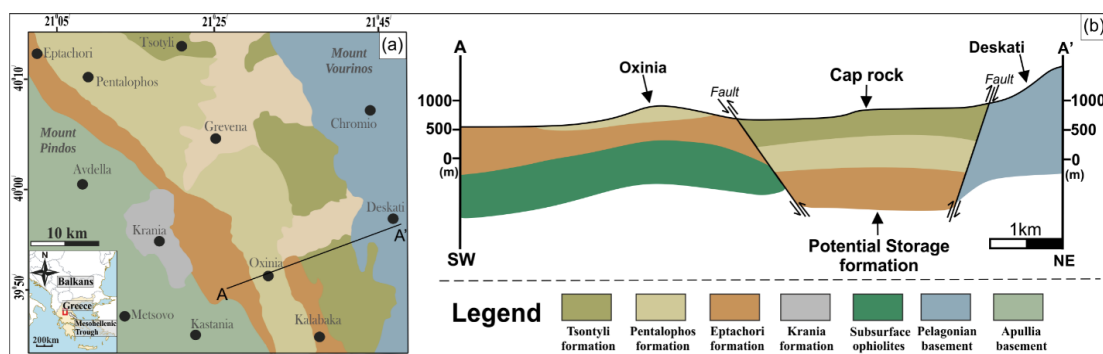


Figure 2. (a) Geological map of the Mesohellenic Trough region, WGS'84 and (b) Cross section displaying the potential site for energy storage purposes.

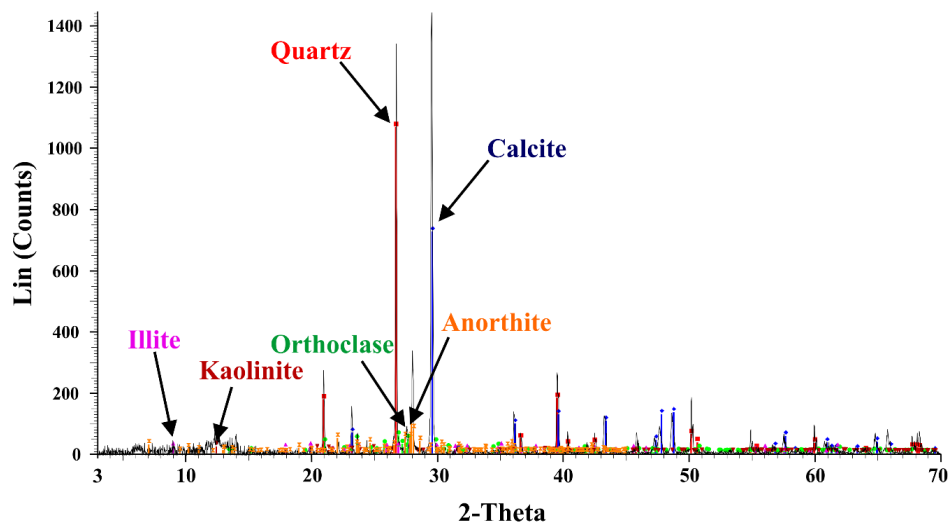
The widespread distribution of Mesohellenic Trough sandstones is usually favoured by their high permeability and geochemical characteristics that provide the potential for long-term pH buffer capacity [59]. High volume sandstones are deformed in open anticline structures representing possible porous reservoir rocks [60]. Sedimentary basins of comparable geological features including the Mesohellenic Trough were considered (Table 1) in the current study. In this frame, all of the other sights examined include a suitable geological reservoir consisting of sandstones that are overlain by Tsotyli formation) caprock [61]. Preliminary investigations were conducted in these sights combined with fieldwork and referenced data provided from the literature. These results showed that all the sandstone formations exhibit comparable textural and mineralogical features, presenting restricted variations in terms of porosity.

Their texture ranges from fine grained to medium grained, displaying variable amounts of sub-angular to sub-rounded lithic fragments and straight to suture grain contacts. It also ranges from poor to moderate sorted presenting high amounts of siliceous cement and local patches of calcareous cement material. Their mineralogical assemblage is composed mainly by quartz, alkali-feldspars, calcite (Figure 3), lithic fragments, mica (mostly muscovite and less frequently biotite) and chlorite (Figure 4c,d). Fragments are mostly composed by quartz and feldspar, as well as by clasts of magmatic origin. Quartz appears in the form of monocrystalline angular or polycrystalline sub-angular to sub-round grains. Quartz contacts are straight, suture or interlocking. K-feldspar occurs in the form of variable sized euhedral to subhedral crystals affected from different weathering degrees. Mica and chlorite appear within the sandstone matrix in the form of scarce occurrences developed intergranular between quartz and feldspar crystals.

Table 1. Thermal Capacity properties of Aquifers from selected localities.

Aquifers Considered	Thermal Capacity (MJ)	Productivity (m ³ /day)	Heat in Place (MJ)
Sappes	3.370	353	3 × 10 ⁻³
Agioi Theodoroi-Komotini	2.930	1193	3 × 10 ⁻³
Mitrikou lake	3.009	788	9 × 10 ⁻⁴
Serres	2.435	11,169	1 × 10 ⁻³
W. Thessaloniki Shallow Thermal	2.382	162	4 × 10 ⁻⁴
W. Thessaloniki-Alexandria	3.577	1516	1 × 10 ⁻³
Mesohellenic Trough_ South Grevena	3.700	57,709	25 × 10 ⁻³
Flysch Botsara syncline	3.822	64,304	18 × 10 ⁻³
Aliveri Evia	2.703	405	1 × 10 ⁻³
Megalopoli	2.291	109	4 × 10 ⁻⁴
Thimiana Chios	3.021	80	5 × 10 ⁻⁴
Lesbos-Thermi	2.885	44.5	2 × 10 ⁻³
Kos	2.394	404	1 × 10 ⁻³
Samos	2.461	37.5	7 × 10 ⁻⁴
Limnos	2.692	38.5	1 × 10 ⁻³
Rhodes	2.249	832	9 × 10 ⁻⁴
Mesohellenic Trough_Felio	4.175	92,747	18 × 10 ⁻³
W. Thessaloniki_ SG	3.93	11,082	7 × 10 ⁻³
W. Thessaloniki_ DG	4.651	3253	1 × 10 ⁻³
Fili landfill_Attica	2.589	4352	1 × 10 ⁻³
North Mesohellenic basin_ SG	3.700	43,282	22 × 10 ⁻³
North Mesohellenic basin_ DG	4.006	93,778	3 × 10 ⁻³

(Data was collected on potential and possible locations for various underground energy storage technologies in aquifers—see Supplementary Table S1 for more details).

**Figure 3.** XRD patterns of Mesohellenic Trough sandstone sample (West Macedonia).

3.3. Pleistocene Alkaline Basalt Occurrences

In Greece, these types of rocks are mostly of Triassic age, having been formed at the stage of oceanic rifting. Localities of these basaltic occurrences include Pindos (NW Greece) [62], Koziakas [63], Othris [64], Argolis [65], the South Aegean [66–68], Volos [3] and Evia Island [69]. Alkaline basalt occurrences of relatively recent age (Pleistocene) appear only in the form of scattered outcrops

mostly in the Aegean Sea (Central Greece). These occurrences outcrop between North Evoikos and Pagasitikos gulfs (Central Greece) and were formed during Pleistocene by extensional back-arc processes associated with the activity of Northern Anatolia Fault [70–72]. These rocks crop out in the islands of Achilleio, Lichades and Agios Ioannis and consist of massive lavas and pyroclastic rocks [3]. In addition, extensional related basaltic rocks also crop out in the regions of Volos, Kamena Vourla and Psathoura (Central Greece) and they are classified as basaltic trachyandesites and trachyandesites [3]. The aforementioned rock types can serve as potential sites for applications of CO₂ storage, which is further enhanced by their relatively low alteration grade. These volcanic centers are not genetically associated with those developed in the South Aegean arc, which resulted from the subduction of the African plate beneath the Eurasia [3,73,74].

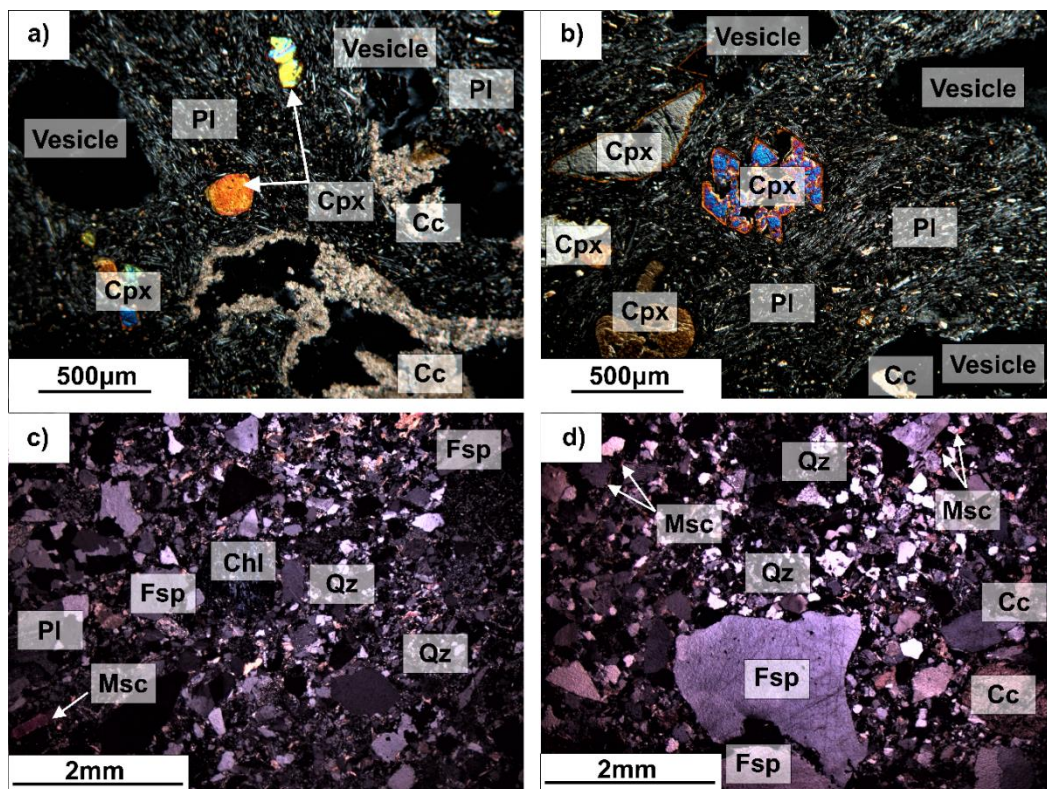


Figure 4. (a,b) Mesohellenic Trough sandstone photomicrographs including feldspar fragments (Fsp) within quartz (Qz) rich groundmass. Calcite (Cc) and muscovite (Ms) appear in the form of accessory minerals. (c,d) Basaltic rock samples presenting porphyritic textures composed by plagioclase (Pl) rich groundmass and clinopyroxene (Cpx) phenocrysts. Gas vesicles have been partially filled with secondary calcite (Cc).

Basaltic rocks from the region of Volos present fine grained holocrystalline trachytic or aphanitic groundmass, characterised from porphyritic vesicular textures (Figure 4a,b) Their mineralogical assemblage is composed mainly by subhedral to euhedral clinopyroxene and olivine phenocrystals (Figure 4a,b). Their groundmass is predominantly composed by needle to lath shaped plagioclase and clinopyroxene crystals (~60%). Accessory minerals include orthopyroxene, alkali-feldspar, amphibole, calcite within gas vesicles, pyrite and opaque oxide minerals such as ilmenite and magnetite.

Clinopyroxene is classified mainly as diopside presenting quite high FeO (FeO: 5.37–8.17 wt.%) and variable TiO₂ and Al₂O₃ contents [3]. Olivine is classified as forsterite presenting higher MgO contents compared to those of FeO, whereas Mg# ranges highly [3]. Plagioclase of the basaltic groundmass is CaO rich classified as bytownite or labradorite, whereas the glassy part is characterised by high SiO₂ and Al₂O₃ and total alkali (Na₂O + K₂O) contents [3].

The vast majority of basaltic samples present porosity within the range of 15%–23% corresponding to 18% average porosity of the studied suite [3]. Their porosity is highly affected from the occurrence of gas vesicles that present variable size range and are usually filled with secondary calcite.

4. Types of Energy and CO₂ Storage Considered

4.1. Underground Thermal Energy Storage (UTES)

4.1.1. Thermal Capacity Properties of Aquifers

The Aquifer Thermal Energy Storage (ATES) is an open loop system that uses permeable water rock layers as means for storing thermal energy and water. Energy can be transferred into or extracted from aquifers using one or more injection and production wells connected with hydraulic pumps and heat exchangers [75]. This technology also can be combined with Geothermal Heat Pumps (GHP). ATES presents the highest energy efficiency compared to other geothermal technologies but strongly depends on the physical properties of the aquifer (thickness, heat capacity). It is also favourable for large-scale energy storage, such as seasonal storage.

In cases where they are overlain by impermeable sedimentary cap rocks (such as siltstones and shales), aquifers can serve as appropriate formations for thermal storage purposes due to their high porosity. In the current study twenty-two geological formations that present the necessary geological, petrological, mineralogical and textural features have been considered for implementation of underground thermal energy storage (Table 1). Thermal capacity, productivity and heat in place are parameters strongly associated with the pore volume and the physicochemical properties of an aquifer media (Table 1). Thermal energy capacity calculations in the studied aquifers was based on the following equation [76] (see Appendix A Table A1):

$$q = (C_p \cdot \rho)_{\text{rock}} \cdot (1 - \varphi) + (C_p \cdot \rho)_{\text{water}} \cdot \varphi \quad (1)$$

Based on referenced data specifications [76] a heat capacity value of 0.19 m (mineral matrix) and an average density of 1.41 kg/m³ were considered as appropriate values for the sandstone aquifers. Results of the current research study indicate that porosity ranges from 8% to 22%, with an average value of 14%. Therefore, the specific thermal capacity per cubic meter for the aquifers considered in the current study is calculated as follows: $q = 2.36 \times 10^{-5} \text{ MJ/m}^3 \cdot ^\circ\text{C}$.

The parameters that have been taken into consideration in order to make our energy storage calculations are transmissivity (Table 2), productivity, porosity, aquifer thickness and permeability. In particular, transmissivity is the product of the aquifer thickness (D) and the average value of hydraulic conductivity (K). It is expressed in m²/day of aquifer thickness [77]. Transmissivity describes an aquifer's capacity to transmit water.

$$T = K \cdot D \quad (2)$$

The productivity of an aquifer depends on its ability to store and transmit water, as well as on the physicochemical characteristics of the geological formation [78]. Productivity is significantly associated with the porosity type, which is classified into primary and secondary [78,79]. In the first case, water is stored within the interstices between grains, whereas secondary porosity refers to the water stored and/or flowing through fractures. Estimation of productivity provides a way to compare the quality of wells from reservoirs with similar properties. Simplified versions of the equations are listed below [80] (see Appendix A Table A1):

$$Q_o = KV1 \cdot Kh \cdot (PF - PS)/VISO \quad (3)$$

$$Q_g = KV2 \cdot Kh \cdot ((PF - PS)^2)/(T + KT2) \quad (4)$$

Heat in place refers to the assessment of the stored heat within a geothermal reservoir. The heat pump potential of geothermal systems can be assessed by estimating the recoverable heat from the total

thermal energy stored in a significant volume of porous and permeable reservoir [81–83]. The thermal extraction rate of a specific reservoir is highly associated with its heat transfer properties affected from the fracture network of the rock mass, as well as the flow regime for heat transfer. The energy stored within a geothermal reservoir is calculated by the following equation [84]:

$$E = \rho \cdot c \cdot V \cdot (T_R - T_{ref}) \quad (5)$$

An alternative calculation for the available heat in place (H) expressed in Joule is provided according to the following equation [85]:

$$H = V_{rock} \cdot P_{rock} \cdot C_{p_{rock}} \cdot (T_z - T_r) \quad (6)$$

Heat injection temperature is associated with the amounts of Underground Thermal Energy storage, as well as with the heat and thermal energy recovery [86]. In the current study, a scenario of injecting 70 °C was considered. The decrease rate of the initially achieved temperature was controlled by two major factors. The first factor includes the temperature distribution in association with the ratio distance of the media, whereas the second concerns the heat loss resulted from the thermal conduction [86,87]. The latter strongly depends on the time period and the initial temperature of the aquifer within the sandstone reservoir. Taking these into consideration, a 70 °C temperature scenario was implemented in every case. The average temperature parameters were applied in Equation (6) also considering the local aquifer and injection temperatures. The expected temperature of an aquifer after the injection of 70 °C is estimated to be ~10 °C warmer. In the case of the “Sappes” aquifer the temperature is 33 °C (Supplementary Table S1). Thus, the temperature to be applied in Equation (1) is estimated 43 °C, which equals to 3.370 MJ thermal capacity.

Table 2. Transmissivity properties of the studied aquifers (see Supplementary Table S1 for more properties).

Aquifers Considered	Transmissivity (m ²)
Aquifer Sappes	6.9×10^{-14}
Aquifer Agioi Theodoroi-Komotinis	2.21×10^{-13}
Aquifer Mitrikou lake	1.77×10^{-13}
Aquifer Serres	4.14×10^{-13}
Aquifer Western Thessaloniki_Shallow Thermal	5.92×10^{-14}
Aquifer_Western Thessaloniki_Alexandria	1.18×10^{-13}
Aquifer_Mesohellenic Trough_South Grevena	1.97×10^{-12}
Aquifer Flysch Botsara syncline	2.96×10^{-13}
Aquifer Aliveri Evia	3.45×10^{-13}
Aquifer Megalopoli	7.89×10^{-14}
Aquifer Thimiana Chios	7.4×10^{-14}
Aquifer Lesbos-Thermi island	5.92×10^{-15}
Aquifer Kos island	6.9×10^{-13}
Aquifer Samos island	2.96×10^{-14}
Aquifer Limnos island	2.96×10^{-14}
Aquifer Rhodes	1.18×10^{-13}
Aquifer_Mesohellenic Trough_Felio	1.48×10^{-12}
Aquifer_Western Thessaloniki_SG	2.96×10^{-13}
Aquifer_Western Thessaloniki_DG	8.29×10^{-14}
Aquifer_Fili landfill_Attica	2.24×10^{-13}
North Mesohellenic basin_SG	1.97×10^{-12}
North Mesohellenic basin_DG	1.48×10^{-12}

A storage system can potentially include more than one reservoir rocks characterised from different physicochemical properties. The content of a reservoir rock can be estimated through direct or

indirect techniques. This can be accomplished via laboratory measurements on core rock samples [88]. The assessment of an explored rock reservoir strongly depends on its mineralogical and chemical composition, coupled with its morphological and sedimentological properties [89].

The studied aquifers of the current research, present thermal capacity values that range between 2.249 and 4.651 MJ. Aquifers of Mesohellenic Trough, Western Thessaloniki basin, as well as the aquifer of Botsara flysch display the best performance regarding their thermal capacity properties (Figure 5). In particular, Mesohellenic Trough aquifers present thermal capacity contents ranging from 3.7 MJ to 4.175 MJ (Table 1). Similar values correspond to the studied aquifers of North Mesohellenic Trough ranging from 3.7 to 4.006 MJ. The aforementioned results indicate that Mesohellenic Trough aquifers exhibit homogeneity regarding their thermal energy properties throughout their whole geographic distribution. On the other hand, aquifers of Western Thessaloniki basin (Figure 5), exhibit a wide range of thermal capacity contents from 2.382 to 4.651 MJ (Table 1).

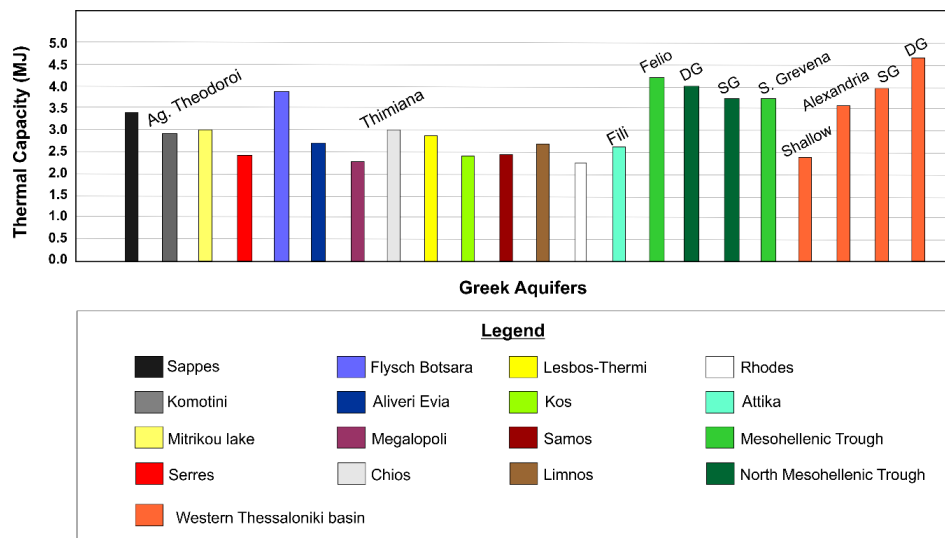


Figure 5. Thermal capacity column chart of the studied Greek aquifers.

4.1.2. UTES Heat Capacity Properties

Underground thermal energy storage (UTES) systems cover a wide range of different technologies including: (a) sensible heat storage that transfers heat to the storage medium or liquid, (b) latent heat storage, where heat is absorbed or released by a phase transition and (c) thermo-chemical storage, in which energy is stored or released through thermochemical reactions.

Assessment of the stored heat is based on numerical-simulation models, providing the potential to address the dynamic changes to the thermal energy as they are affected by recharge and injection processes [90]. The resource volume can change as it shrinks or expands by injection or hot/cold recharge [90]. To quantify these resources it is necessary to determine the amount of the available heat and physicochemical properties of the geothermal rock reservoir [91]. Geothermal resources assessment is based on a volumetric heat content model for porous reservoirs. The heat stored within the rock matrix (index m) and pore water (index w) is calculated by the following equation [92] (see Appendix A Table A1).

$$H = [(1 - P) \cdot \rho_m \cdot C_m + P \cdot \rho_w \cdot C_w] \cdot (T_t - T_o) \cdot A \cdot \Delta z \quad (7)$$

The Area Heat Energy Capacity is calculated by dividing the amount of the Total Heat Energy Capacity with the surface area according to the following equation:

$$\text{Area Heat Energy Capacity (MWh}_{\text{[th]}}/\text{km}^2) = \frac{\text{Total Heat Energy Capacity (MWh}_{\text{[th]}})}{\text{Total Area (km}^2)} \quad (8)$$

Research results of the current study indicate that the Serres, Komotini and Sappes aquifers exhibit the highest average values of total heat energy (Figure 6). In particular, the Serrese aquifer exhibits the highest potential of 6,052,932 MJ, followed by the Komitini (Agioli Theodoroi) and Sappes aquifers with 4,076,831 and 2,172,617 MJ, respectively (Table 3). Comparison between aquifers and abandoned mines in the studied regions indicates that in general aquifers present significantly higher total heat energy capacity compared to that of the abandoned mines. The abandoned coal mine of Aliver (Evia Island; Central Greece) shows the highest potential for underground heat storage (723,255 MJ) compared to that of Chaidari and Mandra in Attica (Central Greece).

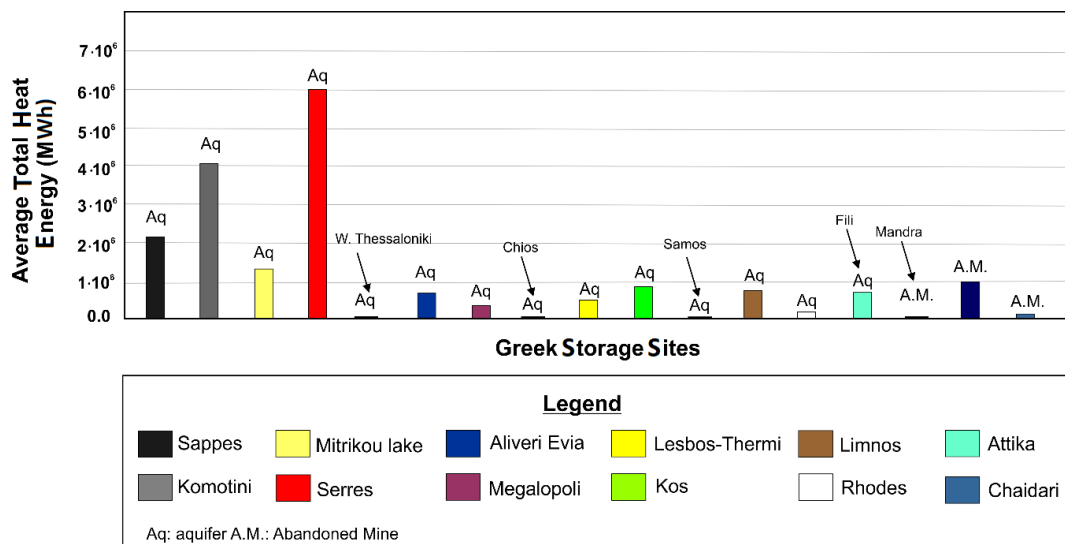


Figure 6. Average total heat energy column chart of the studied Greek aquifers and abandoned mines.

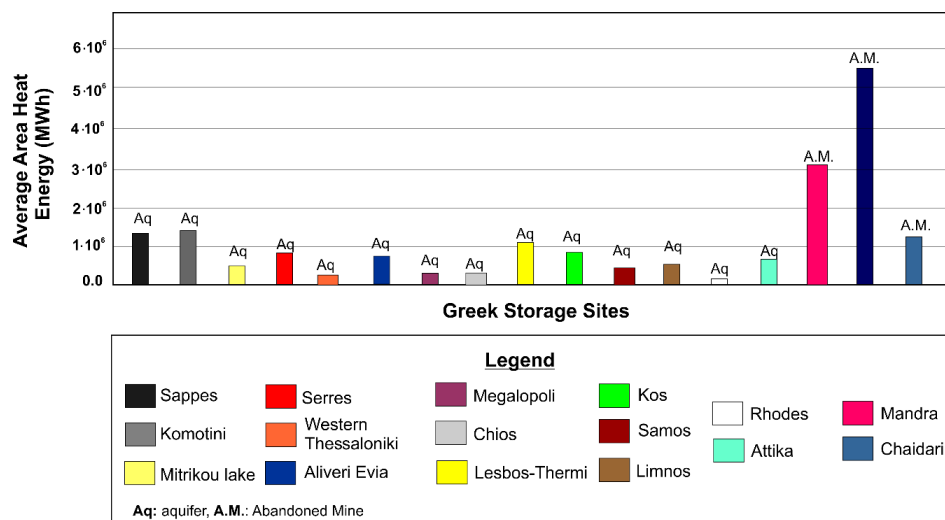
Considering the area average heat values of the studied regions (Table 3), the aquifers tend to exhibit lower values compared to those of abandoned mines, which are significantly higher (Figure 7). In particular, the aquifer average area heat energy ranges from 227,864 to 1,365,479 MJ. The highest values in the studied aquifers correspond to those of Sappes and Komotini (Agioli Theodoroi) regions. Regarding the abandoned mines their average area heat energy ranges from 1,181,993 to 5,440,280 MJ, with the Aliveri abandoned coal mine presenting the highest potential.

The aforementioned results (Table 3) indicate that Aquifer Thermal Energy Storage is one of the most promising technological options that provides large storage capacities [93,94]. By utilising the subsurface space in these sites, Underground Thermal Energy Storage systems potentially provide sustainable heating and cooling energy for different building types. Thus the ATEs integration in a district or urban level can be more efficient compared to a conventional separate heating and cooling generation technology [94,95].

The East Macedonia-Thrace region consumes 3765 kWh per household for electricity needs [96]. In Greece 40% of the total energy consumption corresponds to electricity needs, whereas the 60% corresponds to space heating [97]. Thus, in East Macedonia-Thrace the thermal energy consumption is 5647.5 kWh. Taking these into consideration, it is suggested that the Sappes, Serres and Komotini (Agioli Theodoroi) aquifers (Table 3) could cover the space heating energy consumption of this region.

Table 3. Underground Thermal energy storage systems (UTES) Capacity in selected sites (see Supplementary Table S2 for additional details).

Sites Considered (* Aquifer, ** Abandoned Mine)	Average Total Heat Energy Storage Capacity (MWh _[th])	Average Area Heat Energy Storage Capacity (MWh _[th])
Sappes *	2,172,617	1,284,404
Agioi Theodoroi Komotinis *	4,076,831	1,365,479
Mitrikou lake *	1,335,808	448,048
Serres *	6,052,932	793,685
W. Thessaloniki Shallow Thermal *	13,232	249,200
Aliveri Evia *	723,255	691,274
Megalopoli *	384,557	227,864
Thimiana Chios *	9599	256,027
Lesbos-Thermi *	509,167	1,024,109
Kos *	847,815	836,356
Samos *	21,801	384,041
Limnos *	767,700	473,650
Rhodes *	162,278	477,918
Fili landfill_Attica *	673,119	621,720
Mandra Attica **	34,543	2,997,653
Aliveri **	936,938	5,440,280
Chaidari **	65,198	1,181,993

**Figure 7.** Average area heat energy column chart of the studied Greek aquifers and abandoned mines.

4.2. Underground Gas Storage Potential

Underground gas storage is currently regarded as a mature and widely implemented technology in a global scale. The choice of the appropriate gas reservoir strongly depends on many factors such as [98]: (a) porosity, permeability and storage capacity of the host rock, (b) cap rock occurrence, (c) depth of capture and (d) the physicochemical properties of the underground water.

There are three types of underground natural gas storage at the current stage and these include depleted oil and gas reservoirs, salt-caves and aquifers. Natural gas is injected into the storage regions during the slack season of gas usage (mainly summer) and is produced during the busy season (mainly winter) from storage reservoirs [99]. In depleted natural gas and oil reservoirs conversion of gas/oil field (from production to storage stage) benefits from the existing infrastructure (wells, gathering systems, and pipeline connections), as well as on the massive societal acceptance. These are the most commonly used underground storage types due to their wide availability [100]. The amount of the stored natural

gas strongly depends on the formation porosity and permeability, which affect the natural gas flow rate. The flow rate subsequently affects the rate of injection and withdrawal of working gas [101].

Predictions suggest an increasing energy demand within the following years. Therefore, planned infrastructure projects, in which Greece involves as a transit country, will be developed. These projects include the Trans Adriatic Pipeline (TAP) [102–104] the IGB (Interconnector Greece Bulgaria) gas interconnector between Greece-Bulgaria [103,104] and the EastMed gas pipelines [103] to improve security and diversity of Europe's energy.

Results of the current study (Table 4) indicate that potential sites for implementation of underground gas storage technologies in Greece include gas fields, aquifers and evaporites. In particular, the Prinos and South Kavala gas fields present significantly higher storage capacities compared to the other types presented (aquifers and evaporites; Figure 8). These results further confirm the high storage potential of South Kavala gas field for natural gas storage purposes. The South Kavala Gas field (North Greece) is a promising case for underground gas storage in Greece (Table 4). It is a site with proven feasibility and is expected to be deployed in the following years. The available data show that the cumulative gas production to date is approximately 847 Mm³ (million m³) (Recovery Factor RF 85%) and the estimated remaining gas volume is 148 Mm³, respectively [105]. Evaporite formations are the second most important types presenting storage capacity values ranging from 649,668 to 757,327 MWh_(e). Regarding the studied aquifers, those included in the sedimentary formations of Western Thessaloniki basin and Mesohellenic Trough exhibit the highest potential for underground gas storage.

Taking into consideration that the electricity consumption per household is 3765 kWh for East Macedonia and Thrace [96], it is concluded that the Prinos and S. Kavala gas fields (Table 4) could cover the electricity needs for the households in this region.

Table 4. Underground gas storage (UGS) Capacity in selected sites (see Supplementary Table S3 for additional details).

Sites Considered (* Gas Field, ** Aquifer, *** Salt Structure)	Total Gas Volume (Mm ³)	Working Gas Volume (Mm ³)	Cushion Gas Volume (Mm ³)	Energy Storage Capacity (MWh _(e))
South Kavala *	847	720	127	2,672,920
Epanomi *	500	250	250	928,097
Katakolo *	300	150	150	556,858
Prinos *	2280	1300	980	4,826,105
Western Thessaloniki_ Alexandria **	3	1	2	3712
Mesohellenic Trough_ South Grevena **	44	13	31	48,261
Flysch Botsara syncline **	33	10	23	37,123
Mazarakia ***	281	175	106	649,668
Heraklion ***	328	204	124	757,327
Mesohellenic Trough Filio **	25	8	17	29,699
Western Thessaloniki SG **	136	41	95	152,208
Western Thessaloniki DG **	29	93	20	345,252
North Mesohellenic basin SG **	130	39	91	144,783
North Mesohellenic basin DG **	214	64	150	237,593
Delvinaki ***	218	175	106	649,668

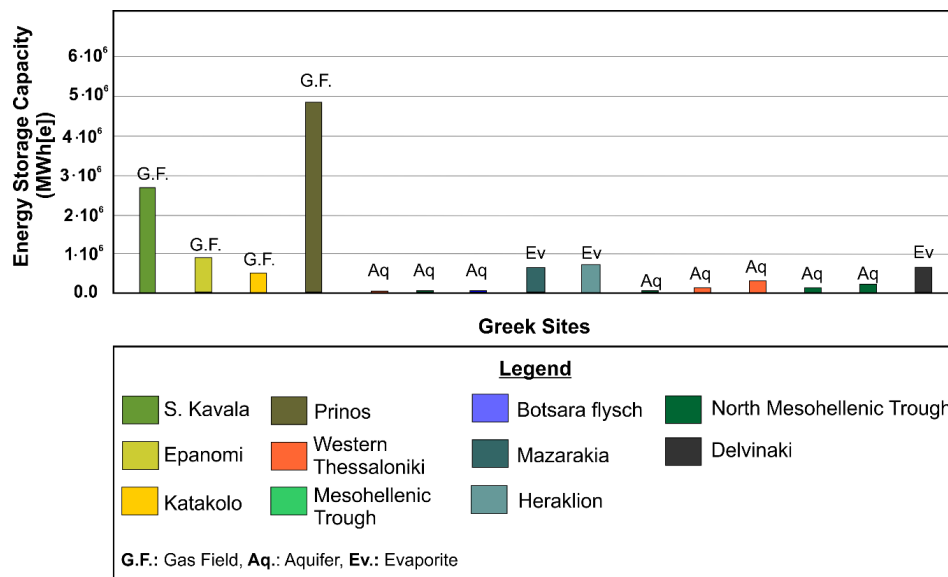


Figure 8. Average energy storage capacity (MWh_e) column chart of the studied Greek aquifers, evaporites and abandoned mines.

4.3. Hydrogen Storage Potential

According to the geological data considered, the potential sites for the development of underground hydrogen storage practices are those of Trifos, Achira (Aitoloakarnania Central-Western Greece), as well as the Kefalonia and Corfu islands. These locations have been already deployed for on-shore wind energy production, whose excess energy can be used to produce hydrogen within an environmentally friendly framework. In order to modelise the potential of storing hydrogen within the aforementioned storage sites a capsule-shaped cavern is assumed as a case scenario. This particular shape is proposed because research studies have shown that these are more stable in terms of stress risks compared to other shapes considered for cavern development [106]. A capsule cavern of elliptical shape was assumed [106]. The cavern volume is 550,000 m³, with diameter of 60 and 300 m height, at a depth of 650 m. The average temperature of hydrogen stored in such evaporite cavern is calculated using Equation (9) [17]:

$$T_{\text{average}} = 288 + 0.025 \times (\text{depth} - \text{cavern height}/2) \quad (9)$$

which is calculated at 27 °C, taking into consideration the geothermal gradient. In this equation, T_{average} stands for average gas temperature of 15 °C, depth in meters and cavern height in meters.

Based on reference data considerations [17,106], an amount of 367,000 m³ as the average working hydrogen volume and an amount of 183,000 m³ for cushion volume were estimated. The working volume refers to the maximum usable storage capacity expressed in energy content. The storage capacity can also be expressed in energy terms and significantly by calculating it in MWh_e. Our case scenario presents comparable features with an already existing hydrogen storage site in Chevron, Texas (USA), which enables the storage of 580,000 m³ hydrogen volume, at 83,300 MWh_(th) energy storage capacity and ~850–1150 m depth [106]. Based on this site specifications it is estimated that our case study presents the potential for 80,000 MWh_(th) energy storage capacity for 650 m depth and 550,000 m³ hydrogen volume. Considering that 1 MWh_e = 1/3 MW_(th) [107], the aforementioned value corresponds to 26,600 MWh_e. This scenario applies for all the above-mentioned sites (Trifos, Achira, Kefalonia and Corfu) that could potentially be deployed.

Taking into consideration that the average electricity consumption of Ionian islands is 3929 kWh per household [96] and the islands of Kefalonia and Corfu can store up to 53,200 MWh_e, it is concluded that hydrogen could cover the electricity needs of 6770 households.

4.4. Recommended CO₂ Storage Sites

Geological CO₂ storage within permeable rock types such as basalts (CarbFix project, Iceland) [27,28] and sandstones [29,30,108] is one of the most efficient technologies for mitigating anthropogenic CO₂ emissions. Enhanced oil recovery provides a crucial option for secure CO₂ storage in oil fields. In this framework several high impact EOR (Enhanced Oil Recovery) projects have been implemented [26,109]. Specific rock types (basalts, sandstones and evaporites) from many Greek regions were considered in the current study regarding their potential for CO₂ storage.

There is a detailed literature regarding the potential of selected Greek regions. Pleistocenic alkaline basaltic outcrops in the region of Volos is considered as a promising site to apply carbon storage [3]. Their abundance in Ca-bearing minerals, low alteration grade and high porosity provide the appropriate physicochemical properties for the implementation of CO₂ storage via mineralisation. Preliminary calculations indicate a storage potential of 82,800 and 27,600 tons of CO₂ maximum mass [3]. The aforementioned indications for implementation of carbon storage are further supported by the indications of enhanced heat based on calculations of groundwater temperatures from irrigation wells. Similar elevated temperatures have been calculated in adjacent regions of Kamena Vourla (Central Greece; East Thessaly) and Lichades Islands (Central Greece; North Evoikos Gulf) [110].

Based on geochemical simulations conducted by [29], presenting reactions within the sandstone brine system of the Mesohellenic Trough it is concluded that the Pentalofos and Tsotyli sedimentary formations could serve as potential sites for long term CO₂ storage produced by the adjacent power plants [29]. The potential of CO₂ storage within sandstone formations is highly affected from the abundance of feldspars and plagioclase crystals [36,111]. Research studies indicate that K-feldspars react with the injected CO₂ producing clay minerals (kaolinite, illite), NaAlCO₃(OH)₂ and K₂CO₃ [36]. Kaolinite precipitation is further enhanced from plagioclase dissolution which also produces considerable amounts of calcite [36]. Further estimations on CO₂ capacity in the Mesohellenic Trough indicate that Pentalofos formation is a geological reservoir formation capped by Tsotyli formation which serves as a cap-rock [37].

Additional sites with potential of CO₂ storage in Greece include the Miocene sandstones of the Prinos and South Kavala regions, at ~1600 m depth with 35 Mt CO₂ storage capacity [19]. The offshore-Prinos basin can host 30 Mt CO₂ within oil reservoirs, as well as 1350 Mt CO₂ in deep saline Miocene aquifers at 2400 m depth [19]. The Epanomi gas field (Figure 1) presents 2 Mt CO₂ capacity within limestones at 2600 m depth, whereas the deep saline aquifers within sedimentary formations of Thessaloniki basin present 640 Mt CO₂ storage capacity at 900–2400 m depth [19]. In South Greece the Katakolo oil and gas field could serve as potential site for CO₂ storage purposes within the Cretaceous-Eocene limestones presenting 3.2 Mt CO₂ capacity [19].

Based on the aforementioned literature data, in combination with additional key parameters guidelines are proposed suggesting which perspective sites are most suitable for CO₂ storage: (a) Mesohellenic Trough sandstones, (b) Volos basalts, (c) Western Thessaloniki saline aquifers and (d) depleted gas field of Prinos. These parameters include the geographical distribution of the regions, the CO₂ storage techniques that can be implemented, as well as the possibility to develop cost-effective scenarios.

The Volos basalts, the Mesohellenic Trough and the Western Thessaloniki basin are located close to industrial regions, indicating that CO₂ storage can be favoured by reduced costs of transport. These industrial regions include the cities of (a) Volos (10 km distance from the corresponding basalt occurrences), (b) Grevena, Ptolemais, Kozani (which lie close to the Mesohellenic Trough sandstones) and (c) Thessaloniki (which is located at the geographical boundaries of Western Thessaloniki basin). The implementation of CO₂ storage within Mesohellenic Trough sandstones through combination of geological storage (within the permeable Tsotilli and Pentalofos formations), or carbon mineralisation, provides significant advantages compared to the other regions.

Concerning the case of the depleted oil reservoir in the off-shore Prinos basin, the relatively high storage capacity coupled with the use of existing infrastructures, suggests that storage of CO₂ can

be implemented in a cost-effective framework. In addition, the capability of such reservoirs to host hydrocarbons deposits for long time periods minimises risks for safety hazards associated with CO₂ containment compared to other sites [112]. Deep saline aquifers often include water of unsuitable quality for agricultural and drinking water usage [21]. Thus, the aquifers of Western Thessaloniki basin present significant advantage to be exploited for CO₂ storage.

5. Conclusions

This study presents, maps and investigates several Greek regions regarding their capacity on underground thermal energy storage (UTES), underground gas storage (UGS), hydrogen storage and CO₂ storage. To achieve that preliminary results and petrographical data were presented and compared with literature data. The main concluding remarks are:

- Thermal energy capacity was examined in 22 sandstone aquifers throughout several regions of Northern, Central Greece and Aegean islands. Research results indicate that the aquifers of Mesohellenic Trough, Western Thessaloniki basin and those of Botsara flysch exhibit the highest thermal capacity values, which can reach up to 4175 MJ.
- Heat capacity was investigated in 14 aquifers throughout the Northern and Southern Greece, as well as on three abandoned mines from Attica region and Aliveri regions (Central Greece). In general, the aquifers tend to present higher average total heat energy values that reach up to $\sim 6.05 \times 10^6$ MWh_(th) compared to those of the abandoned mines. In particular, the Sappes, Serres and Komotini (Agioi Theodoroi) aquifers could cover the space heating energy consumption of East Macedonia-Thrace region.
- Underground gas storage technologies present better performance in the gas fields of South Kavala and Prinos basins compare to the studied evaporite formations and aquifers. These two gas fields could cover the electricity needs of the households in the region of East Macedonia and Thrace.
- Hydrogen storage capacity was based on a capsule-shaped cavern scenario in Trifos and Achira regions (Central-Western Greece), as well as in Kefalonia and Corfu islands. Calculations indicate storage capacity of 26,600 MWh_(e) for each of the studied regions. These calculated hydrogen capacity values for Corfu and Kefalonia islands, could efficiently cover the electricity needs of 6770 households in the Ionian Sea region.
- Petrological studies of the Mesohellenic trough sandstones coupled with basaltic rocks from Volos region (Central Greece) indicate that these rocks could serve as potential sites for CO₂ storage via CO₂-mineralisation. This is attributed to their high porosity, low alteration grade and abundance on Fe–Mg–Ca–K silicate minerals.
- Based on CO₂ capacity data provided by the literature, geographical distribution criteria, potential for implementation of CO₂ storage techniques and cost-considerations, we recommend the: (a) Volos basalts, (b) Mesohellenic trough sandstones, (c) saline aquifers of Western Thessaloniki basin and (d) the oil reservoir of Prinos basin, as the most promising sites for CO₂ storage in Greece.

Supplementary Materials: The following are available online at <http://www.mdpi.com/1996-1073/13/11/2707/s1>, Table S1: Prop (Properties), Table S2: Assess_UGS, Table S3: Assess_H2, Table S4: Assess_Therm (Thermal Capacity), Table S5: Coordinates.

Author Contributions: Conceptualization, A.A. and P.K.; Investigation, A.A., P.K., N.K., P.T., D.K. and C.K.; Methodology, A.A., P.K., D.K. and C.K.; Supervision, A.A., P.K. and N.K.; Validation, D.K. and P.P.; Writing—original draft, A.A., P.K., N.K., P.T., D.K., C.K. and P.P. All authors have read and agreed to the published version of the manuscript.

Funding: This research received no external funding.

Acknowledgments: We would like to express our sincerest thanks to the Reviewers and the Editor for their constructive comments that substantially helped to improve the current paper. The preliminary research results provided in this paper were published in the frame of the EU Horizon 2020-funded program ESTMAP. Many thanks are also given to Georgia Kastanioti (Geologist) and Pavlos Krassakis (Geologist) for their participation of the previously mentioned EU Horizon 2020-funded project.

Conflicts of Interest: The authors declare no conflict of interest.

Appendix A

Table A1. Symbology, description of symbols and units used in equations presented in this study.

Symbol	Description	Unit
Cp	heat capacity	MJ/kg·°C
rho	dry bulk density	kg/m ³
phi	porosity	%
T	transmissivity	m ² /day
K	hydraulic conductivity	m/day
D	aquifer thickness	m
Kh	permeability-thickness product	m ² -m
PFa	average formation pressure	Pa
T	temperature	°C
VISO	oil viscosity	mm ² /s
Qg	productivity gas	m ³ /day
c	volumetric specific heat of the reservoir rock	MJ/kg·°C
V	volume of the reservoir	m ³
TR	the characteristic reservoir temperature	°C
TREF	the reference temperature	°C
H	heat in place	MJ
Vrock	the denoting rock volume	m ³
Prock	the rock density	kg/m ³
H	total heat energy storage capacity	MJ
P	effective porosity	%
ρm	density of the rock matrix	kg/m ³
ρw	density of water	kg/m ³
cm	specific heat capacity of the rock matrix	MJ/kg·°C
cw	specific heat capacity of water	MJ/kg·°C
Tt	mean temperature of the compartment	°C
A	surface area under consideration	m ²
Δz	aquifer thickness	m
Taverage	average temperature of stored hydrogen	°C
depth	depth	m
cavernHeight	height of the cavern	m
	KV1 = 7.5 × 10 ⁻⁶ m ³ /day	
	KV2 = 1 × 10 ⁻⁵ m ³ /day	
	Density of water: 997 kg/m ³	
	Density of rock matrix (e.g., sandstone): 2323 kg/m ³	

References

1. Davis, W. The Relationship between Atmospheric Carbon Dioxide Concentration and Global Temperature for the Last 425 Million Years. *Climate* **2017**, *5*, 76. [[CrossRef](#)]
2. IPCC. *Climate Change 2013: The Physical Science Basis. Contribution of Working Group I to the Fifth Assessment Report of the Intergovernmental Panel on Climate Change*; Cambridge University Press: New York, NY, USA, 2013; p. 1535.
3. Koukouzas, N.; Koutsovitis, P.; Tyrologou, P.; Karkalis, C.; Arvanitis, A. Potential for Mineral Carbonation of CO₂ in Pleistocene Basaltic Rocks in Volos Region (Central Greece). *Minerals* **2019**, *9*, 627. [[CrossRef](#)]

4. Rosenbauer, R.J.; Thomas, B.; Bischoff, J.L.; Palandri, J. Carbon sequestration via reaction with basaltic rocks: Geochemical modeling and experimental results. *Geochim. Cosmochim. Acta* **2012**, *89*, 116–133. [[CrossRef](#)]
5. Bott, C.; Dressel, I.; Bayer, P. State-of-technology review of water-based closed seasonal thermal energy storage systems. *Renew. Sustain. Energy Rev.* **2019**, *113*, 109241. [[CrossRef](#)]
6. Montcoudiol, N.; Burnside, N.M.; Györe, D.; Mariita, N.; Mutia, T.; Boyce, A. Surface and groundwater hydrochemistry of the Menengai Caldera Geothermal Field and surrounding Nakuru County, Kenya. *Energies* **2019**, *12*, 3131. [[CrossRef](#)]
7. Xu, X.; Wei, Z.; Ji, Q.; Wang, C.; Gao, G. Global renewable energy development: Influencing factors, trend predictions and countermeasures. *Resour. Policy* **2019**, *63*, 101470. [[CrossRef](#)]
8. Nataraj Barath, J.G.; Husev, O.; Manonmani, N. Overview of Energy Storage Technologies For Renewable Energy. *IJISET* **2015**, *2*, 6.
9. Mofijur, M.; Mahlia, T.M.I.; Silitonga, A.S.; Ong, H.C.; Silakhori, M.; Hasan, M.H.; Putra, N.; Rahman, S.A. Phase Change Materials (PCM) for Solar Energy Usages and Storage: An Overview. *Energies* **2019**, *12*, 3167. [[CrossRef](#)]
10. Dincer, I.; Rosen, M. *Thermal Energy Storage: Systems and Applications*; John Wiley & Sons: Hoboken, NJ, USA, 2010.
11. Paksoy, H.Ö.; Beyhan, B. Thermal energy storage (TES) systems for greenhouse technology. In *Advances in Thermal Energy Storage Systems. Methods and Applications*; Cabeza, L.F., Ed.; Woodhead Publishing, Elsevier: Cambridge, UK, 2015; p. 612.
12. De Schepper, G.; Paulus, C.; Bolly, P.-Y.; Hermans, T.; Lesparre, N.; Robert, T. Assessment of short-term aquifer thermal energy storage for demand-side management perspectives: Experimental and numerical developments. *Appl. Energy* **2019**, *242*, 534–546. [[CrossRef](#)]
13. Park, J.-W.; Rutqvist, J.; Ryu, D.; Park, E.-S.; Synn, J.-H. Coupled thermal-hydrological-mechanical behavior of rock mass surrounding a high-temperature thermal energy storage cavern at shallow depth. *Int. J. Rock Mech. Min. Sci.* **2016**, *83*, 149–161. [[CrossRef](#)]
14. Arvanitis, A. Investigation of the Possibilities for the Subsurface Energy Storage in the frame of the EC-funded ESTMAP Project. In Proceedings of the 11th National Conference on Renewable Energy Sources, Thessaloniki, Greece, 14–16 March 2018.
15. Breeze, P. Power System Energy Storage Technologies. In *Power Generation Technologies*, 3rd ed.; Breeze, P., Ed.; Elsevier Ltd.: Amsterdam, The Netherlands, 2019; pp. 219–249.
16. Lemieux, A.; Sharp, K.; Shkarupin, A. Preliminary assessment of underground hydrogen storage sites in Ontario, Canada. *Int. J. Hydrog. Energy* **2019**, *44*, 15193–15204. [[CrossRef](#)]
17. Caglayan, D.; Weber, N.; Heinrichs, H.; Linszen, J.; Robinius, M.; Kukla, P.; Stolten, D. Technical potential of salt caverns for hydrogen storage in Europe. *Int. J. Hydrog. Energy* **2020**, *45*, 6793–6805. [[CrossRef](#)]
18. Crotagino, F.; Donadei, S.; Bünger, U.; Landinger, H. Large-Scale Hydrogen Underground Storage for Securing Future Energy Supplies. In Proceedings of the 18th World Hydrogen Energy Conference, Essen, Germany, 16–21 May 2010.
19. Arvanitis, A.; Koukouzas, N.; Koutsovitis, P.; Karapanos, D.; Manoukian, E. Combined CO₂ Geological Storage and Geothermal Energy Utilization in Greece. In Proceedings of the 15th International Congress of the Geological Society of Greece Harokopio University of Athens, Athens, Greece, 22–24 May 2019.
20. Hasan, M.M.F.; Boukouvala, F.; First, E.L.; Floudas, C.A. Nationwide, Regional, and Statewide CO₂ Capture, Utilization, and Sequestration Supply Chain Network Optimization. *Ind. Eng. Chem. Res.* **2014**, *53*, 7489–7506. [[CrossRef](#)]
21. Celia, M.A.; Bachu, S.; Nordbotten, J.M.; Bandilla, K.W. Status of CO₂ storage in deep saline aquifers with emphasis on modeling approaches and practical simulations. *Water Resour. Res.* **2015**, *51*, 6846–6892. [[CrossRef](#)]
22. Jalili, P.; Saydam, S.; Cinar, Y. CO₂ Storage in Abandoned Coal Mines. In Proceedings of the Underground Coal Operators' Conference Wollongong, Wollongong, Australia, 10–11 February 2011; p. 410.
23. Xie, L.Z.; Zhou, H.; Xie, H. Research advance of CO₂ storage in rock salt caverns. *Yantu Lixue/Rock Soil Mech.* **2009**, *30*, 7.
24. Baran, P.; Zarębska, K.; Krzystalik, P.; Hadro, J.; Nunn, A. CO₂-ECBM and CO₂ sequestration in Polish coal seam—Experimental study. *J. Sustain. Min.* **2014**, *13*, 22–29. [[CrossRef](#)]

25. Raza, A.; Gholami, R.; Rezaee, R.; Bing, C.H.; Nagarajan, R.; Hamid, M.A. Well selection in depleted oil and gas fields for a safe CO₂ storage practice: A case study from Malaysia. *Petroleum* **2017**, *3*, 167–177. [[CrossRef](#)]
26. Györe, D.; Stuart, F.M.; Gilfillan, S.M.V.; Waldron, S. Tracing injected CO₂ in the Cranfield enhanced oil recovery field (MS, USA) using He, Ne and Ar isotopes. *Int. J. Greenh. Gas Control* **2015**, *42*, 554–561. [[CrossRef](#)]
27. Snæbjörnsdóttir, S.Ó.; Wiese, F.; Fridriksson, T.; Ármansson, H.; Einarsson, G.M.; Gislason, S.R. CO₂ storage potential of basaltic rocks in Iceland and the oceanic ridges. *Energy Procedia* **2014**, *63*, 4585–4600. [[CrossRef](#)]
28. Ragnheidardóttir, E.; Sigurdardóttir, H.; Kristjansdóttir, H.; Harvey, W. Opportunities and challenges for CarbFix: An evaluation of capacities and costs for the pilot scale mineralization sequestration project at Hellisheidi, Iceland and beyond. *Int. J. Greenh. Gas Control* **2011**, *5*, 1065–1072. [[CrossRef](#)]
29. Koukouzas, N.; Kypridou, Z.; Purser, G.; Rochelle, C.A.; Vasilatos, C.; Tsoukalas, N. Assessment of the impact of CO₂ storage in sandstone formations by experimental studies and geochemical modeling: The case of the Mesohellenic Trough, NW Greece. *Int. J. Greenh. Gas Control* **2018**, *71*, 116–132. [[CrossRef](#)]
30. Garcia-Rios, M.; Luquot, L.; Soler, J.; Cama, J. Laboratory-Scale Interaction between CO₂-Rich Brine and Reservoir Rocks (Limestone and Sandstone). *Procedia Earth Planet. Sci.* **2013**, *7*, 109–112. [[CrossRef](#)]
31. Boschi, C.; Dini, A.; Dallai, L.; Ruggieri, G.; Gianelli, G. Enhanced CO₂-mineral sequestration by cyclic hydraulic fracturing and Si-rich fluid infiltration into serpentinites at Malenrata (Tuscany, Italy). *Chem. Geol.* **2009**, *265*, 209–226. [[CrossRef](#)]
32. Dichicco, M.C.; Laurita, S.; Paternoster, M.; Rizzo, G.; Sinisi, R.; Mongelli, G. Serpentine Carbonation for CO₂ Sequestration in the Southern Apennines: Preliminary Study. *Energy Procedia* **2015**, *76*, 477–486. [[CrossRef](#)]
33. Bennaceur, K. CO₂ Capture and Sequestration. In *Future Energy*, 2nd ed.; Letcher, T.M., Ed.; Elsevier: Amsterdam, The Netherlands, 2014; pp. 583–611.
34. Piessens, K.; Duser, M. CO₂-sequestration in abandoned coal mines. In Proceedings of the International Coalbed Methane Symposium, Tuscaloosa, AL, USA, 5–8 May 2003; p. 11.
35. Kelektoglou, K. Carbon Capture and Storage: A Review of Mineral Storage of CO₂ in Greece. *Sustainability* **2018**, *10*, 4400. [[CrossRef](#)]
36. Petrounias, P.; Giannakopoulou, P.; Rogkala, A.; Kalpogiannaki, M.; Koutsovitis, P.; Damoulianou, M.-E.; Koukouzas, N. Petrographic Characteristics of Sandstones as a Basis to Evaluate Their Suitability in Construction and Energy Storage Applications. A Case Study from Klepa Nafpaktias (Central Western Greece). *Energies* **2020**, *13*, 1119. [[CrossRef](#)]
37. Tasiannas, A.; Koukouzas, N. CO₂ storage capacity estimate in the lithology of the Mesohellenic Trough, Greece. *Energy Procedia* **2016**, *86*, 334–341. [[CrossRef](#)]
38. Koukouzas, N.; Gemeni, V.; Zioc, H.J. Sequestration of CO₂ in magnesium silicates, in Western Macedonia, Greece. *Int. J. Miner. Process.* **2009**, *93*, 179–186. [[CrossRef](#)]
39. ESTMAP, Energy Storage Mapping and Planning Home Page. Available online: <http://estmap.eu/deliverables.html> (accessed on 5 May 2020).
40. Karakitsios, V. Western Greece and Ionian Sea petroleum systems. *AAPG Bull.* **2013**, *97*, 1567–1595. [[CrossRef](#)]
41. Karakitsios, V.; Rigakis, N. Evolution and petroleum potential of Western Greece. *J. Pet. Geol.* **2007**, *30*, 197–218. [[CrossRef](#)]
42. Tserolas, P.; Mpotziolis, C.; Maravelis, A.; Zelilidis, A. Preliminary Geochemical and Sedimentological Analysis in NW Corfu: The Miocene Sediments in Agios Georgios Pagon. In Proceedings of the 14th International Congress of Geological Society of Greece, Thessaloniki, Greece, 25–27 May 2016; pp. 402–411.
43. Karakitsios, V.; Roveri, M.; Lugli, S.; Manzi, V.; Gennari, R.; Antonarakou, A.; Triantaphyllou, M.; Agiadi, K.; Kontakiotis, G.; Kafousia, N.; et al. A Record of the Messinian Salinity Crisis in the Eastern Ionian Tectonically Active Domain (Greece, Eastern Mediterranean). *Basin Res.* **2017**, *29*, 203–233. [[CrossRef](#)]
44. Kokinou, E.; Kamberis, E.; Kotsi, F.; Lioni, K.; Velaj, T. The Impact of Evaporites in the Greek and Albanian Oil Systems. In Proceedings of the 79th EAGE Conference and Exhibition 2017, Paris, France, 12–15 June 2017.
45. Velaj, T. The structural style and hydrocarbon exploration of the subthrust in the Berati Anticlinal Belt, Albania. *J. Pet. Explor. Prod. Technol.* **2015**, *5*, 123–145. [[CrossRef](#)]
46. Velaj, T. Tectonic style in Western Albania Thrustbelt and its implication on hydrocarbon exploration. *AAPG Search Discov. Artic.* **2011**, 123–148.

47. Kontopoulos, N.; Zelilidis, A.; Piper, D.J.W.; Mudie, P.J. Messinian evaporites in Zakynthos, Greece. *Palaeogeogr. Palaeoclimatol. Palaeoecol.* **1997**, *129*, 361–367. [[CrossRef](#)]
48. Bourli, N.; Kokkaliari, M.; Iliopoulos, I.; Pe-Piper, G.; Piper, D.J.W.; Maravelis, A.G.; Zelilidis, A. Mineralogy of siliceous concretions, cretaceous of ionian zone, western Greece: Implication for diagenesis and porosity. *Mar. Pet. Geol.* **2019**, *105*, 45–63. [[CrossRef](#)]
49. Tsipoura-Vlachou, M. Diagenesis of the Marly-Gypsum Formations, Igoumenitsa Area, N.W. Greece. *Bull. Geol. Soc. Greece* **2007**, *40*, 1009–1021. [[CrossRef](#)]
50. Getsos, K.; Papaioannou, F.; Zelilidis, A. Triassic Carbonate and Evaporite Sedimentation in the Ionian Zone (Western Greece): Palaeogeographic and Palaeoclimatic Implication. *Bull. Geol. Soc. Greece* **2004**, *36*, 699–707. [[CrossRef](#)]
51. Flugel, E. Mikrofazielle Untersuchungen in der Alpenen Trias: Methoden and Probleme. *Mitt. Ges. Geol. Bergbaustud.* **1972**, *21*, 9–64.
52. Vamvaka, A.; Spiegel, C.; Frisch, W.; Danisik, M. Fission track data from the Mesohellenic Trough and the Pelagonian zone in NW Greece: Cenozoic tectonics and exhumation of source areas. *Int. Geol. Rev.* **2010**, *52*, 223–248. [[CrossRef](#)]
53. Rassios, A.; Moores, E. Heterogeneous mantle complex, crustal processes, and obduction kinematics in a unified Pindos-Vourinos ophiolitic slab (northern Greece). *Geol. Soc. Lond. Spec. Publ.* **2006**, *260*, 237–266. [[CrossRef](#)]
54. Kiliadis, A.; Vamvaka, A.; Falalakis, G.; Sfeikos, A.; Papadimitriou, E.; Gkarlaouuni, C.; Karakostas, B. The Mesohellenic Trough and the Paleogene Thrace Basin on the Rhodope Massif, their Structural Evolution and Geotectonic Significance in the Hellenides. *J. Geol. Geosci.* **2015**, *4*, 2. [[CrossRef](#)]
55. Brunn, J.H. Contribution à l'étude géologique du Pinde septentrional et d'une partie de la Macédoine occidentale. *Ann. Géol. Pays Hell.* **1956**, *8*, 346–358.
56. Papanikolaou, D.; Lekkas, E.; Mariolagos, H.; Mirkou, R. Contribution on the geodynamic evolution of the Mesohellenic trough. *Bull. Geol. Soc. Greece* **1988**, *20*, 17–36.
57. Aubouin, J. Contribution à l'étude géologique de la Grèce septentrionale: Le confins de l'Épire et de la Thessalie. *Ann. Géol. Pays Hell.* **1959**, *10*, 525.
58. Koukouzas, C.; Koukouzas, N. Coals of Greece: Distribution, quality and reserves. *Geol. Soc. Spec. Publ.* **1995**, *82*, 171–180. [[CrossRef](#)]
59. Wilson, M.; Monea, M. IEA GHG Weyburn CO₂ monitoring and storage project: Summary report 2000–2001. In Proceedings of the 7th International Conference Greenhouse Gas Control Technology (GHGT-7), Vancouver, BC, Canada, 5–9 September 2005.
60. Koukouzas, N.; Ziogou, F.; Gemeni, V. Preliminary assessment of CO₂ geological storage opportunities in Greece. *Int. J. Greenh. Gas Control* **2009**, *3*, 502–513. [[CrossRef](#)]
61. Tasianas, A.; Koukouzas, N. Assessing the Potential of the Mesohellenic Trough and Other Sites, in Greece, for CO₂ Storage. *Procedia Earth Planet. Sci.* **2015**, *15*, 607–612. [[CrossRef](#)]
62. Saccani, E.; Photiades, A. Mid-ocean ridge and supra-subduction affinities in the Pindos ophiolites (Greece): Implications for magma genesis in a forearc setting. *Lithos* **2004**, *73*, 229–253. [[CrossRef](#)]
63. Pomonis, P.; Tsikouras, B.; Hatzipanagiotou, K. Geological evolution of the Koziakas ophiolitic complex (W. Thessaly, Greece). *Ophioliti* **2005**, *30*, 77–86.
64. Koutsovitis, P. Gabbroic rocks in ophiolitic occurrences from East Othris, Greece: Petrogenetic processes and geotectonic environment implications. *Mineral. Petrol.* **2011**, *104*, 249–265. [[CrossRef](#)]
65. Saccani, E.; Beccaluva, L.; Photiades, A.; Zeda, O. Petrogenesis and tectono-magmatic significance of basalts and mantle peridotites from the Albanian–Greek ophiolites and sub-ophiolitic mélanges. New constraints for the Triassic–Jurassic evolution of the Neo-Tethys in the Dinaride sector. *Lithos* **2011**, *124*, 227–242. [[CrossRef](#)]
66. Stouraiti, C.; Pantziris, I.; Vasilatos, C.; Kanellopoulos, C.; Mitropoulos, P.; Pomonis, P.; Moritz, R.; Chiaradia, M. Ophiolitic Remnants from the Upper and Intermediate Structural Unit of the Attic-Cycladic Crystalline Belt (Aegean, Greece): Fingerprinting Geochemical Affinities of Magmatic Precursors. *Geosciences* **2017**, *7*, 14. [[CrossRef](#)]
67. Mortazavi, M.; Sparks, R. Origin of rhyolite and rhyodacite lavas and associated mafic inclusions of Cape Akrotiri, Santorini: The role of wet basalt in generating calcalkaline silicic magmas. *Contrib. Mineral. Petrol.* **2004**, *146*, 397–413. [[CrossRef](#)]

68. Bachmann, O.; Deering, C.; Ruprecht, J.; Huber, C.; Skopelitis, A.; Schnyder, C. Evolution of silicic magmas in the Kos-Nisyros volcanic center, Greece: A petrological cycle associated with caldera collapse. *Contrib. Mineral. Petrol.* **2012**, *163*, 151–166. [[CrossRef](#)]
69. Pe-Piper, G.; Panagos, A.G. Geochemical characteristics of the Triassic volcanic rocks of Evia: Petrogenetic and tectonic implications. *Ofioliti* **1989**, *14*, 33–50.
70. Pe-Piper, G.; Piper, D. Neogene backarc volcanism of the Aegean: New insights into the relationship between magmatism and tectonics. *Geol. Soc. Am.* **2007**, *418*, 17–31. [[CrossRef](#)]
71. Fytikas, M.; Innocenti, F.; Manetti, P.; Peccerillo, A.; Mazzuoli, R.; Villari, L. Tertiary to Quaternary evolution of volcanism in the Aegean region: The Geological Evolution of the Eastern Mediterranean. In *Geological Society Special Publication*; Dixon, J.E., Robertson, A.H.F., Eds.; The Geological Society Publishing House: Bath, UK, 1984; Volume 17, pp. 687–699.
72. Innocenti, F.; Agostini, S.; Doglioni, C.; Piero, M.; Tonarini, S. Geodynamic evolution of the Aegean: Constraints from the Plio-Pleistocene volcanism of the Volos-Evia area. *J. Geol. Soc. Lond.* **2010**, *167*, 475–489. [[CrossRef](#)]
73. Nicholls, I.A. Petrology of Santorini Volcano, Cyclades, Greece. *J. Petrol.* **1971**, *12*, 67–119. [[CrossRef](#)]
74. Nicholls, I.A. Santorini volcano, greece—Tectonic and petrochemical relationships with volcanics of the Aegean region. *Tectonophysics* **1971**, *11*, 377–385. [[CrossRef](#)]
75. Bridger, D.W.; Allen, D.M. Designing aquifer thermal energy storage systems. *ASHRAE J.* **2005**, *47*, S32.
76. Vance, D. Heat in Groundwater Systems Part I—The Fundamentals. *Natl. Environ. J.* **1996**, *6*, 30–31.
77. Brandt, M.J.; Johnson, K.M.; Elphinston, A.J.; Ratnayaka, D.D. *Twort's Water Supply*, 7th ed.; Elsevier: Amsterdam, The Netherlands, 2017.
78. Maidment, D.R. *Handbook of Hydrology*; McGraw-Hill: New York, NY, USA, 1992.
79. Price, M. *Introducing Groundwater*, 2nd ed.; Chapman and Hall: London, UK, 1996.
80. Crain, E.R. *Crain's Petrophysical Handbook*; Spectrum 2000 Mindware: Rocky Mountain House, AB, Canada, 1987.
81. Nathanson, M. *Physical Factors Determining the Fraction of Stored Energy Recoverable from Hydrothermal Convection Systems and Conduction-Dominated Areas*; U.S. Geological Survey Open-File Report: Menlo Park, CA, USA, 1975; p. 50.
82. White, D.E.; Williams, D.L. *Assessment of Geothermal Resources of the United States*; U.S. Geological Survey Circular: Arlington, VA, USA, 1975; p. 155.
83. Muffler, L.J.P. *Assessment of Geothermal Resources of the United States*; U.S. Geological Survey Circular: Roosevelt, UT, USA, 1979; p. 163.
84. Franco, A.; Donatini, F. Methods for the estimation of the energy stored in geothermal reservoirs. *J. Phys. Conf. Ser.* **2017**, *796*, 012025. [[CrossRef](#)]
85. Beardsmore, G.; Rybach, L.; Blackwell, D.; Baron, C. A Protocol for Estimating and Mapping Global EGS Potential. *GRC Trans.* **2010**, *34*, 301–312.
86. Gao, L.; Zhao, J.; An, Q.; Liu, X.; Du, Y. Thermal performance of medium-to-high-temperature aquifer thermal energy storage systems. *Appl. Therm. Eng.* **2019**, *146*, 898–909. [[CrossRef](#)]
87. Van Lopik, J.H.; Hartog, N.; Jan Zaadnoordijk, W. The use of salinity contrast for density difference compensation to improve the thermal recovery efficiency in high-temperature aquifer thermal energy storage systems. *Hydrogeol. J.* **2016**, *24*, 1255–1271. [[CrossRef](#)]
88. Berger, B.; Anderson, K. *Modern Petroleum: A Basic Primer of the Industry*, 3rd ed.; Pennwell Books: Houston, TX, USA, 1992; p. 517.
89. North, F.K. *Petroleum Geology*; Allen & Unwin: Boston, MA, USA, 1985.
90. Franz, P.; Neville-Lamb, M.; Azwar, L.; Quinao, J. Calculation of Geothermal Stored Heat from a Numerical Model for Reserve Estimation. In *Proceedings of the World Geothermal Congress, Melbourne, Australia, 19–25 April 2015*.
91. Muffler, P.; Cataldi, R. Methods for regional assessment of geothermal resources. *Geothermics* **1978**, *7*, 53–89. [[CrossRef](#)]
92. Schellschmidt, R.; Hurter, S. Atlas of Geothermal Resources in Europe. *Geothermics* **2003**, *32*, 779–787. [[CrossRef](#)]

93. Pellegrini, M.; Bloemendal, M.; Hoekstra, N.; Spaak, G.; Andreu Gallego, A.; Rodriguez Comins, J.; Grotenhuis, T.; Picone, S.; Murrell, A.J.; Steeman, H.J. Low carbon heating and cooling by combining various technologies with Aquifer Thermal Energy Storage. *Sci. Total Environ.* **2019**, *665*, 1–10. [\[CrossRef\]](#)
94. Todorov, O.; Alanne, K.; Virtanen, M.; Kosonen, R. A method and analysis of aquifer thermal energy storage (ATES) system for district heating and cooling: A case study in Finland. *Sustain. Cities Soc.* **2020**, *53*, 101977. [\[CrossRef\]](#)
95. Hooimeijer, F.; Maring, L. The significance of the subsurface in urban renewal. *IRPUS* **2018**, *11*, 303–328. [\[CrossRef\]](#)
96. Kostakis, I. Socio-demographic determinants of household electricity consumption: Evidence from Greece using quantile regression analysis. *CRSUST* **2020**, in press. [\[CrossRef\]](#)
97. Azeiteiro, U.; Davim, J. *Higher Education and Sustainability*, 1st ed.; CRC Press: Boca Raton, FL, USA, 2020.
98. Tichler, R.; Bauer, S. Power to gas. In *Storing Energy with Special Reference to Renewable Energy Sources*; Letcher, T.M., Ed.; Elsevier: Oxford, UK, 2016; p. 590.
99. Renpu, W. Basis of Well Completion Engineering. In *Advanced Well Completion Engineering*, 3rd ed.; Renpu, W., Ed.; Gulf Professional Publishing: Oxford, UK, 2011; pp. 1–74.
100. Speight, J.G. Recovery, storage, and transportation. In *Natural Gas*, 2nd ed.; Speight, J.G., Ed.; Gulf Professional Publishing: Boston, MA, USA, 2019; pp. 149–186.
101. Speight, J.G. (Ed.) Reservoirs and Reservoir Fluids. In *Handbook of Hydraulic Fracturing*; Wiley: Hoboken, NJ, USA, 2016; pp. 27–54.
102. Papadopoulou, D.; Tourkoulis, C.N.; Mirasgedis, S. Assessing the macroeconomic effect of gas pipeline projects: The case of Trans-Adriatic Pipeline on Greece. *SPOUIDAI* **2015**, *65*, 100–118.
103. Khalova, G.O.; Illeritskiy, N.I.; Smirnova, V.A. Prospects for the Construction of the Poseidon Gas Pipeline as a Factor in Supplying the Needs of the Southern Europe Countries with Natural Gas. *Int. J. Energy Econom. Policy* **2019**, *9*, 143–148.
104. Kotek, P.; Granado, P.C.d.; Egging, R.; Toth, B.T. European Natural Gas Infrastructure in the Energy Transition. In Proceedings of the 16th International Conference on the European Energy Market (EEM), Ljubljana, Slovenia, 18–20 September 2019; pp. 1–6.
105. Kitsilis, M.-C. Issues for Underground Gas Storage (UGS) in ‘South Kavala’ offshore gas field. In Proceedings of the 5th South East Europe Energy Dialogue, Thessaloniki, Greece, 2–3 June 2011.
106. Ozarslan, A. Large-scale hydrogen energy storage in salt caverns. *Int. J. Hydrog. Energy* **2012**, *37*, 14265–14277. [\[CrossRef\]](#)
107. Winter, C.-J.; Nitch, J. *Hydrogen as an Energy Carrier: Technologies, Systems, Economy*; Springer: Stuttgart, Germany, 1988.
108. Eiken, O.; Ringrose, P.; Hermanrud, C.; Nazarian, B.; Torp, T.A.; Høier, L. Lessons learned from 14 years of CCS operations: Sleipner, In Salah and Snøhvit. *Energy Procedia* **2011**, *4*, 5541–5548. [\[CrossRef\]](#)
109. Beaubien, S.E.; Jones, D.G.; Gal, F.; Barkwith, A.K.A.P.; Braibant, G.; Baubron, J.-C.; Ciotoli, G.; Graziani, S.; Lister, T.R.; Lombardi, S.; et al. Monitoring of near-surface gas geochemistry at the Weyburn, Canada, CO₂-EOR site, 2001–2011. *Int. J. Greenh. Gas Control* **2013**, *16*, S236–S262. [\[CrossRef\]](#)
110. Andritsos, N.; Arvanitis, A.; Papachristou, M.; Fytikas, M.; Dalabakis, P. Geothermal Activities in Greece During 2005–2009. In Proceedings of the World Geothermal Congress Bali, Bali, Indonesia, 25–29 April 2010; pp. 25–29.
111. Jin, C.; Liu, L.; Yiman, I.; Zeng, R. Capacity assessment of CO₂ storage in deep saline aquifers by mineral trapping and the implications for Songliao Basin, Northeast China. *Energy Sci. Eng.* **2017**, *5*, 81–89. [\[CrossRef\]](#)
112. Hannis, S.; Lu, J.; Chadwick, A.; Hovorka, S.; Kirk, K.; Romanak, K.; Pearce, J. CO₂ storage in depleted or depleting oil and gas fields: What can we learn from existing projects? *Energy Procedia* **2017**, *114*, 5680–5690. [\[CrossRef\]](#)

